Application of a Tetra-TPD-type HTM Fused by a Tröger's Base Core in Perovskite Solar Cells

Titas Braukyla, Rui Xia, Tadas Malinauskas, Maryte Daskeviciene, Artiom Magomedov, Egidijus Kamarauskas, Vygintas Jankauskas, Zhaofu Fei, Cristina Roldán-Carmona, Mohammad Khaja Nazeeruddin, Paul J. Dyson* and Vytautas Getautis**

T. Braukyla, Dr. T. Malinauskas, Dr. M. Daskeviciene, A. Magomedov, Prof. V. Getautis
Department of Organic Chemistry, Kaunas University of Technology, Radvilenu pl. 19, 50254, Kaunas, Lithuania
E-mail: vytautas.getautis@ktu.lt

Dr. R. Xia, Dr. C. Roldán-Carmona, Prof. M. K. Nazeeruddin
Group for Molecular Engineering of Functional Materials, Institute of Chemical Sciences and Engineering, École Polytechnique Fédérale de Lausanne, Rue de l'Industry 17, CH-1951, Sion, Switzerland
E-mail: mdkhaja.nazeeruddin@epfl.ch

Dr. R. Xia
State Key laboratory of PV Science and Technology, Trina Solar, Changzhou, 213031 China

Dr. R. Xia, Dr. Z. Fei, Prof. P. J. Dyson.
Institut des Sciences et Ingénierie Chimiques, Ecole Polytechnique Fédérale de Lausanne (EPFL), CH-1015 Lausanne, Switzerland.
E-mail: paul.dyson@epfl.ch

Dr. E. Kamarauskas, Prof. V. Jankauskas
Institute of Chemical Physics Vilnius University, Sauletekio al. 3, Vilnius LT-10257, Lithuania

Keywords: perovskite solar cells, hole transporting materials, Tröger's base

One of the obstacles to the commercialization of perovskite solar cells (PSCs) is the high price and morphological instability of the most common hole-transporting material (HTM) Spiro-OMeTAD. In this work, a novel HTM, termed **V1160**, based on four *N*,*N*′-bis(3-methylphenyl)-*N*,*N*′-diphenylbenzidine (TPD)-type fragments, fused by a Tröger's base core,

was synthesized and successfully applied in PSCs. Investigation of the optical, thermal, and photoelectrical properties showed that **V1160** is a suitable candidate for application as a HTM in PSCs. A promising power conversion efficiency (PCE) of over 18% was demonstrated, which is only slightly lower than that of Spiro-OMeTAD. Moreover, **V1160**-based devices exhibit improved performances in dopant-free configurations and superior stability. Favorable morphological properties in combination with a simple synthesis makes **V1160** and related materials promising for HTM applications.

Over the last decade, perovskite solar cells (PSCs) have emerged as a promising technology rapidly evolving to a level where they rival more established photovoltaic materials.[1-14] Currently, state-of-the-art PSCs have not only outperformed the dye-sensitized solar cells [4,15–17] and organic solar cells, [18–21] but have recently surpassed power-conversion efficiencies (PCEs) of the current market-dominating polycrystalline silicon cells,[22–25] having exceeded a PCE of 24%.[26] The high performance of PSCs may be attributed to the favorable properties of the perovskite absorber layer, such as a high absorption coefficient over the visible and near-infrared range,[27,28] low exciting binding energy,[29] high conductivity and charge carrier mobility,[30–32] long carrier diffusion length in the µm range [33] (1 µm in thin films [34] and up to 175 µm in single crystals [35]), and a tunable band gap by replacing the cations and anions in the perovskite structure. Most of the high-efficiency PSCs reported to date are based on the small organic molecule HTM 2,2`,7,7`-tetrakis(*N*,*N*-di-*p*-methoxy-phenylamine)-9,9`-spirobifluorene (Spiro-OMeTAD), which has become the “gold standard” in PSCs, and PCEs achieved with it have rarely been exceeded by other HTM materials.[2] Unfortunately, the synthesis of Spiro-OMeTAD requires five steps, that require sensitive (*n*-butyllithium or Grignard reagents) and aggressive (Br_2) reagents, and low temperatures (-78 °C) are required making it costly. [36] Indeed, the high cost of Spiro-OMeTAD is a bottleneck for cheap device

production.[31,37,38] Another drawback of Spiro-OMeTAD is its high tendency to crystallize in the device, thus impairing the performance of the cell.[39,40]

The relationship between the structural features of Spiro-OMeTAD and its high efficiency as a HTM offers some insights for designing alternative compounds. Spiro-OMeTAD is conceptually derived from a spiro center perpendicularly conjoining two *p*-methoxy-substituted tetra-*N*-phenylbenzidine compounds, which share the structural skeleton with TPD.[41] TPD and its related compounds are well developed and investigated and used in various optoelectronic devices. Among other applications, TPD is commonly used as HTM in phosphorescent organic light-emitting diodes, especially those employing triplet emitters [42–45]. *p*-Methoxy-substituents found in these TPD-type fragments offer lower ionization potentials (5.4 eV in un-substituted TPD),[46] making them more energetically compatible in PSCs, as well as having improved layer interactions *via* anchoring to hybrid lead iodide perovskites [47]. TPD is also known to have hole drift mobility as high as 1.1 10^{-3} cm^2 V^{-1} s^{-1}, but unfortunately it lacks thermal and morphological stability and tends to readily crystallize, i.e. its T_g is as low as 65 °C.[48] These limitations are also partially noticeable in Spiro-OMeTAD, and could potentially be overcome by finding an alternative to spiro carbon as the connecting and orienting core, and conjoining TPD-type moieties in a different fashion. Tröger's base (TB) can serve this role as a functional core, allowing the synthesis of HTMs with decent properties and high charge mobility.[49] The V-shaped structure of TB provides an angle orientation for the conjugated π-systems attached to it and the rigidity of the TB scaffold (as the high molecular mass via its 2-fold functionalization) impairs crystallization, making the TB derivatives highly amorphous and endowing them with significantly increased glass transition temperatures.[41,50,51]

In this work, we report the synthesis and characterization of **V1160** (**Scheme 1(a)**), having twin-TPD-type fragments fused into each side of TB core, functionally making it a fused-

tetra-TPD-type molecule. **V1160** is further demonstrated to serve as an efficient HTM in triple-cation[52] perovskite-based PSCs based on a n-i-p architecture.

V1160 was synthesized in a straightforward way, with the intermediates obtained following previously reported procedures, starting from the commercially available precursors. The final compound was obtained in high yield utilizing Buchwald-Hartwig amination conditions (**Scheme 1(b)**). After purification, **V1160** was isolated as a slightly colored, amorphous powder, soluble in common organic solvents (e.g. THF, toluene, $CHCl_3$). The structure of **V1160** was confirmed using ^{1}H and ^{13}C NMR spectroscopy and elemental analysis (see SI for full details).

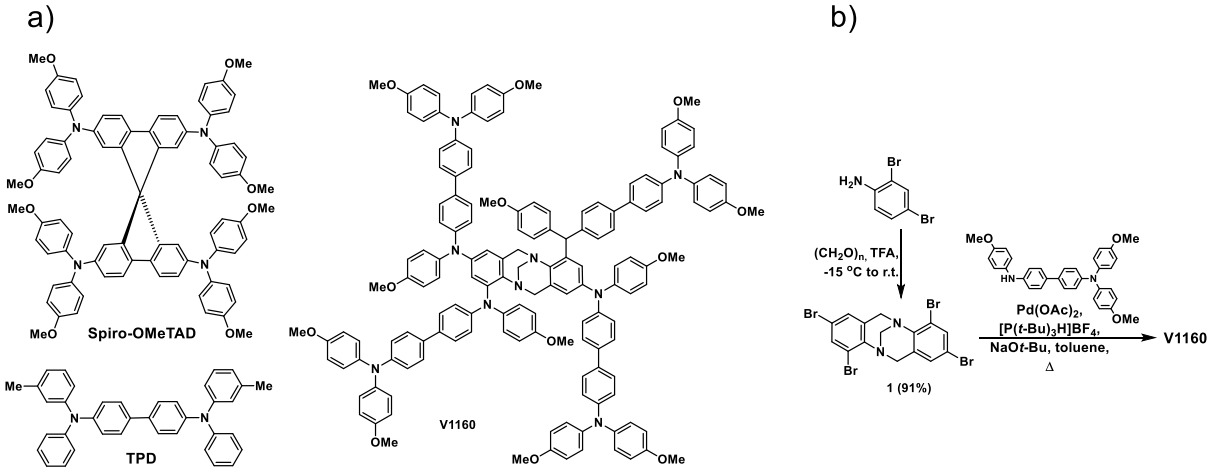

Scheme 1. (a) Molecular structures of the Spiro-OMeTAD, TPD, and the new HTM **V1160**; (b) Synthesis of the **V1160**.

As mentioned above, it is important to obtain fully amorphous HTM film to obtain good long-term stability of a PSC. Therefore, differential scanning calorimetry (DSC) was used to study the phase transitions of the **V1160**. During the first heating cycle (10 K min^{-1}) no melting transition was detected, and only a glass transition (T_g) temperature can be observed (**Figure 1(a)**). During the cooling stage, no crystallization occurred, and on the second heating scan, a T_g value of 166 °C was observed, which is significantly higher than that of Spiro-OMeTAD (124 °C).[39] The absence of a crystalline phase for **V1160** makes this material an attractive candidate for the stable PSC fabrication, as failure due to the crystallization is switched off. In

addition, the thermal stability of **V1160** was evaluated by thermogravimetric analysis (TGA) to reveal stabilty up to the 420 °C, which is compatible with practical applications in optoelectronic devices.

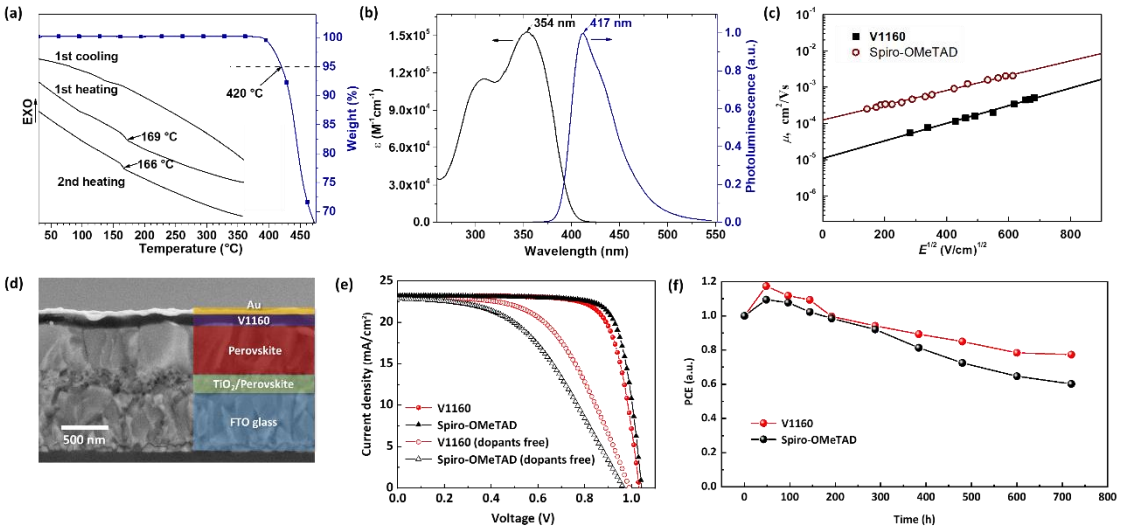

Figure 2. (a) DSC (black lines) and TGA (blue line) analysis of **V1160**; (b) UV/vis absorption (black line) and normalized PL (blue line) spectra of **V1160** in THF; (c) hole-drift mobility measurements of **V1160** and Spiro-OMeTAD;(d) Cross-sectional SEM image of the **V1160**-based device; (e) Current density-voltage (J/V) characteristics under reverse scan of the PSCs with **V1160** and Spiro-OMeTAD as HTMs in the absence and presence of dopants. Scan speed 100 mV s^{-1}; (f) Stability measurements of representative **V1160**- and Spiro-OMeTAD-based devices.

A UV/vis absorption spectrum of **V1160** were recorded in THF (**Figure 1(b)**). **V1160** mostly absorbs light in the UV range (up to ~410 nm) with the absorption maximum (λ_{max}) at 354 nm. The photoluminescence spectrum of**V1160** in THF shows a single asymmetric peak, with an emission maximum (λ_F) of 435 nm, Stokes shift of 63 nm and quantum yield of 37%. To investigate the position of the energy levels of **V1160**, photoelectron spectroscopy in air (PESA) of the HTM film was performed. The solid-state ionization potential value (I_p) was measured as 5.24 eV. This value suggests that **V1160** is compatible with the perovskite (valence band edge – 5.6–5.8 eV)[53–55] energy levels, ensuring good charge extraction. The ability of **V1160** to transport holes was evaluated by measuring xerographic time-of-flight (XTOF) hole drift mobilities. As can be seen from **Figure 1(c)**, for **V1160**, the hole drift

mobility is 1.1×10^{-5} $cm^2\,V^{-1}\,s^{-1}$ at low electrical fields (μ_0), and 9.4×10^{-4} $cm^2\,V^{-1}\,s^{-1}$ at a field strength of $6.4\cdot10^5$ $V\,cm^{-1}$ (μ). For Spiro-OMeTAD these values are 1.2×10^{-4} and 5.2×10^{-3} $cm^2\,V^{-1}\,s^{-1}$, respectively. Despite having a high amount of TPD-type moieties fused in the TB core, **V1160** demonstrated lower μ and μ_0 values. Such behavior can be attributed to the higher disorder in the molecular structure due to the bulky nature of the molecule, interfering with the favorable arrangement with adjacent molecules, and leading to the absence of the crystalline state.

To investigate the performance of **V1160** as a HTM, PSCs with FTO/ compact TiO_2/ mesoporous TiO_2/ amorphous SnO_2/ $[(FAPbI_3)_{0.87}(MAPbBr_3)_{0.13}]_{0.92}(CsPbI_3)_{0.08}$/ HTM/ Au device architecture were constructed, utilizing state-of-the-art "triple-cation"[54] perovskite composition. To fabricate the cells, **V1160** was dissolved in chlorobenzene, with the addition of the dopants, and spin-coated directly on top of the perovskite film (see SI for the detailed procedure). First, the quality of the formed HTM layer was analyzed by recording a cross-sectional scanning electron microscopy (SEM) image of the device (**Figure 1(d)**) which shows that **V1160** forms a film with the thickness of ~110 nm. In addition, top-view SEM images of the perovskite film (**Figure S3(a)**, inset) and HTM-covered perovskite film (**Figure S3(a)**) were recorded. It is evident that the multi-crystalline perovskite film, with an average grain size of around 200 nm, was homogeneously covered by the **V1160** layer.

To evaluate the capacity of the HTM to extract the photo-generated holes, steady-state PL measurements were conducted. Perovskite films prepared on glass were excited at a wavelength of 600 nm and the quenching effect was analyzed in comparison with the pristine perovskite. Results are shown in **Figure S4(a)** and show a higher quenched emission for **V1160** than for Spiro-OMeTAD, suggesting a better hole extracting capability, as expected from their energy levels presented in **Figure S4(b)** (**V1160** $_{HOMO}$ = -5.26 eV vs. Spiro-OMeTAD $_{HOMO}$ = -5.22 eV).[56] In addition, a slight blue shift is observed for the perovskite film covered with **V1160** HTM. Such behavior can be attributed to the interaction between

perovskite and HTM layer[57] and, as a consequence, reduction of the interfacial trap states at the perovskite/HTM contact[58].

PSCs with the **V1160** HTM has a maximum PCE of 18.3%, extracted from the reverse scan of J/V characteristic of the best performing device (**Figure 1(c)**, **Table 1**). Such a value is comparable with that of the reference Spiro-OMeTAD-based PSCs (19.2%), obtained in the same series of batches. The main parameter leading to the slightly lower performance of the **V1160**-based devices corresponds to the fill factor (*FF*), which in this case is 76.6% (78.9% for Spiro-OMeTAD-based device). Such behavior can be attributed to non-optimal charge transport through the HTM film and originates either from the lower hole-drift mobility values or from the worse compatibility with the doping procedure employed. Best open-circuit voltage (V_{oc}) values are very close for these two materials, being only slightly lower for the **V1160**-based PSC (1033 mV vs. 1045 mV for the reference device). Also, the short-circuit current density (J_{sc}) values are almost identical for devices based on both materials (23.09 mA/cm^2 and 23.23 mA/cm^2 for **V1160** and reference PSCs, respectively), which is further confirmed by the incident photon-to-current conversion efficiency (IPCE) measurements, shown in **Figure 1(e)** (values obtained by integration of the IPCE spectra are 22.79 mA/cm^2 for **V1160**-based and 23.07 mA/cm^2 for the reference devices). Even though **V1160** exhibits lower hole-drift mobility, the comparable performance achieved in PSCs could be attributed to the advantageous interface with perovskite surface, as was shown by the PL measurements. In addition, thinner films of ~150 nm (Spiro-OMeTAD standard: ~200 nm) were used to partially compensate losses due to the suboptimal transport of charges through the HTM film.

Table 1. Performance parameters of the PSCs extracted from the J/V characteristics.

HTM	J_{sc} [mA/cm^2]	V_{oc} [mV]	*FF* [%]	PCE [%]
V1160 (Reverse)	23.09	1033	76.6	18.27
V1160 (Forward)	23.06	1032	69.6	16.55
V1160 (Dopants free)	23.02	990	55.3	12.61

Reference (Reverse)	23.23	1045	78.9	19.16
Reference (Forward)	23.20	1039	77.0	18.56
Reference (Dopants free)	22.83	972	46.8	10.39

To obtain a better representation of the **V1160**-based devices, average performance parameters are shown in **Figure S1**, based on data from 20 devices. The spread in the results is low with an average PCE of 17.5±0.36 %. Detailed data for individual cells can be found in the SI.

In addition, the **V1160** HTM was tested in a dopant-free configuration. As dopants are known to chemically interact with the HTMs,[59–61] it is advisable to search for the compounds that ensure sufficient performance without the use of additives. Interestingly, a device with dopant-free **V1160** showed better performance than that of the corresponding Spiro-OMeTAD-based device, resulting in a moderate PCE of 12.6%.

Finally, initial assessment of the **V1160**-based PSC stability was performed by storing non-encapsulated devices in a dark atmosphere with a relative humidity of 45% and periodically tested under 100 mW/ cm^2 simulated sun irradiation (AM 1.5G). Comparison of the results with those of the Spiro-OMeTAD-based system is presented in **Figure 1(f)**. For both materials, an initial increase in performance during the first 50 hours is observed, which is slightly more pronounced in the case of **V1160**, and can be attributed to the slow oxygen-mediated doping process.[62,63] Over time, the efficiency slowly reduces and the device with the **V1160** HTM showed better stability with ~78% of the initial performance maintained after >700 h compared to a drop to 59% for the control device. Such behavior is suggesting that some of the degradation modes (e.g. crystallization of the film under operational conditions[39]) are strongly diminished in the case of **V1160**, which can be attributed to the lower likelihood of **V1160** to crystallize.

In conclusion, we have demonstrated a promising new HTM material, i.e. **V1160**, prepared via a relatively straightforward synthesis with a performance close to that of Spiro-OMeTAD

when applied in PSCs. **V1160** combines four TPD-type fragments in a single molecule via TB bridges. The new HTM demonstrated good performance in PSCs, with the average PCE of 17.5% and record PCE of 18.3%. In addition, **V1160** does not possess a crystalline state, which is essential to achieve stable performance. We believe that applied synthetic strategies can be further utilized for the synthesis of even more efficient and stable HTMs.

Supporting Information

Supporting Information is available from the Wiley Online Library or from the authors.

Acknowledgements

T.B. and R.X. contributed equally to this work. The research leading to these results had received funding from the European Union's Horizon 2020 research and innovation programme under grant agreement No. 763977 of the PerTPV project

Received: ((will be filled in by the editorial staff))
Revised: ((will be filled in by the editorial staff))
Published online: ((will be filled in by the editorial staff))

References

[1] H. J. Snaith, *Nat. Mater.* **2018**, *17*, 372–376.

[2] P. Vivo, J. K. Salunke, A. Priimagi, *Materials (Basel).* **2017**, *10*, 1087.

[3] J.-P. Correa-Baena, M. Saliba, T. Buonassisi, M. Grätzel, A. Abate, W. Tress, A. Hagfeldt, *Science* **2017**, *358*, 739–744.

[4] N. J. Jeon, H. Na, E. H. Jung, T.-Y. Yang, Y. G. Lee, G. Kim, H.-W. Shin, S. Il Seok, J. Lee, J. Seo, *Nat. Energy* **2018**, *3*, 682–689.

[5] S. Collavini, S. F. Völker, J. L. Delgado, *Angew. Chem. Int. Ed.* **2015**, *54*, 9757–9759.

[6] N.-G. Park, M. Grätzel, T. Miyasaka, K. Zhu, K. Emery, *Nat. Energy* **2016**, *1*, 16152.

[7] S. F. Völker, S. Collavini, J. L. Delgado, *ChemSusChem* **2015**, *8*, 3012–3028.

[8] M. Saliba, M. Saliba, T. Matsui, K. Domanski, J.-Y. Seo, A. Ummadisingu, *Science (80-.).* **2016**, *354*, 206–209.

[9] W. Zhang, Y. Wang, X. Li, C. Song, L. Wan, K. Usman, J. Fang, *Adv. Sci.* **2018**, *5*, 1800159.

[10] T. T. Ngo, I. Suarez, G. Antonicelli, D. Cortizo-Lacalle, J. P. Martinez-Pastor, A. Mateo-Alonso, I. Mora-Sero, *Adv. Mater.* **2017**, *29*, 1604056.

[11] S. Paek, P. Qin, Y. Lee, K. T. Cho, P. Gao, G. Grancini, E. Oveisi, P. Gratia, K. Rakstys, S. A. Al-Muhtaseb, *Adv. Mater.* **2017**, *29*, 1606555.

[12] V. D'innocenzo, G. Grancini, M. J. P. Alcocer, A. R. S. Kandada, S. D. Stranks, M. M. Lee, G. Lanzani, H. J. Snaith, A. Petrozza, *Nat. Commun.* **2014**, *5*, 3586.

[13] J. Huang, C. Wang, Z. Liu, X. Qiu, J. Yang, J. Chang, *J. Mater. Chem. C* **2018**, *6*, 2311.

[14] Y. Peng, Y. Cheng, C. Wang, C. Zhang, H. Xia, K. Huang, S. Tong, X. Hao, J. Yang, *Org. Electron.* **2018**, *58*, 153.

[15] M. Pazoki, U. B. Cappel, E. M. J. Johansson, A. Hagfeldt, G. Boschloo, *Energy Environ. Sci.* **2017**, *10*, 672–709.

[16] A. Abate, M. Saliba, W. Tress, T. J. Jacobsson, M. Gr, A. Hagfeldt, *Energy Environ. Sci.* **2017**, *10*, 710–727.

[17] W. Ghann, H. Kang, T. Sheikh, S. Yadav, T. Chavez-Gil, F. Nesbitt, J. Uddin, *Sci. Rep.* **2017**, *7*, 41470.

[18] N. Liang, W. Jiang, J. Hou, Z. Wang, *Mater. Chem. Front.* **2017**, *1*, 1291–1303.

[19] S. D. Collins, N. A. Ran, M. C. Heiber, T. Nguyen, *Adv. Energy Mater.* **2017**, *7*, 1602242.

[20] Y. Ma, Z. Kang, Q. Zheng, *J. Mater. Chem. A* **2017**, *5*, 1860–1872.

[21] G. Li, W.-H. Chang, Y. Yang, *Nat. Rev. Mater.* **2017**, *2*, 17043.

[22] X. Li, D. Bi, C. Yi, J.-D. Décoppet, J. Luo, S. M. Zakeeruddin, A. Hagfeldt, M. Grätzel, *Science* **2016**, *353*, 58.

[23] N. J. Jeon, J. H. Noh, W. S. Yang, Y. C. Kim, S. Ryu, J. Seo, S. Il Seok, *Nature* **2015**,

517, 476–480.

[24] D. P. McMeekin, G. Sadoughi, W. Rehman, G. E. Eperon, M. Saliba, M. T. Hörantner, A. Haghighirad, N. Sakai, L. Korte, B. Rech, et al., *Science* **2016**, *351*, 151.

[25] D. Bi, W. Tress, M. I. Dar, P. Gao, J. Luo, C. Renevier, K. Schenk, A. Abate, F. Giordano, J.-P. C. Baena, *Sci. Adv.* **2016**, *2*, e1501170.

[26] National Renewable Energy Laboratory (NREL), "Best Research-Cell Efficiency Chart," **2019**.

[27] H.-S. Kim, C.-R. Lee, J.-H. Im, K.-B. Lee, T. Moehl, A. Marchioro, S.-J. Moon, R. Humphry-Baker, J.-H. Yum, J. E. Moser, et al., *Sci. Rep.* **2012**, *2*, 418–425.

[28] N.-G. Park, *J. Phys. Chem. Lett.* **2013**, *4*, 2423–2429.

[29] S. Park, J. H. Heo, C. H. Cheon, H. Kim, S. H. Im, H. J. Son, *J. Mater. Chem. A* **2015**, *3*, 24215–24220.

[30] O. Malinkiewicz, A. Yella, Y. H. Lee, G. M. Espallargas, M. Graetzel, M. K. Nazeeruddin, H. J. Bolink, *Nat. Photonics* **2014**, *8*, 128–132.

[31] S. Kazim, M. K. Nazeeruddin, M. Grätzel, S. Ahmad, *Angew. Chem. Int. Ed.* **2014**, *53*, 2812–2824.

[32] J. Burschka, A. Dualeh, F. Kessler, E. Baranoff, N.-L. Cevey-Ha, C. Yi, M. K. Nazeeruddin, M. Grätzel, *J. Am. Chem. Soc.* **2011**, *133*, 18042–18045.

[33] G. Xing, N. Mathews, S. Sun, S. S. Lim, Y. M. Lam, M. Grätzel, S. Mhaisalkar, T. C. Sum, *Science* **2013**, *342*, 344–347.

[34] S. D. Stranks, G. E. Eperon, G. Grancini, C. Menelaou, M. J. P. Alcocer, T. Leijtens, L. M. Herz, A. Petrozza, H. J. Snaith, *Science* **2013**, *342*, 341–344.

[35] Q. Dong, Y. Fang, Y. Shao, P. Mulligan, J. Qiu, L. Cao, J. Huang, *Science* **2015**, *347*, 967–970.

[36] T. P. I. Saragi, T. Spehr, A. Siebert, T. Fuhrmann-Lieker, J. Salbeck, *Chem. Rev.* **2007**, *107*, 1011–1065.

[37] Z. Yu, L. Sun, *Adv. Energy Mater.* **2015**, *5*, 1500213.

[38] H. Kim, K.-G. Lim, T.-W. Lee, *Energy Environ. Sci.* **2016**, *9*, 12–30.

[39] T. Malinauskas, D. Tomkute-Luksiene, R. R. Sens, M. Daskeviciene, R. Send, H. Wonneberger, V. Jankauskas, I. Bruder, V. Getautis, *ACS Appl. Mater. Interfaces* **2015**, *7*, 11107–11116.

[40] S. Ma, H. Zhang, N. Zhao, Y. Cheng, M. Wang, Y. Shen, G. Tu, *J. Mater. Chem. A* **2015**, *3*, 12139–12144.

[41] I. Neogi, S. Jhulki, M. Rawat, R. S. Anand, T. J. Chow, J. N. Moorthy, *RSC Adv.* **2015**, *5*, 26806–26810.

[42] J. Fang, D. Ma, *Appl. Phys. Lett.* **2003**, *83*, 4041–4043.

[43] J. Fang, H. You, J. Gao, D. Ma, *Chem. Phys. Lett.* **2004**, *392*, 11–16.

[44] Z. R. Hong, C. S. Lee, S. T. Lee, W. L. Li, S. Y. Liu, *Appl. Phys. Lett.* **2003**, *82*, 2218–2220.

[45] Y. Tao, C. Yang, J. Qin, *Chem. Soc. Rev.* **2011**, *40*, 2943–2970.

[46] D.-H. Lee, Y.-P. Liu, K.-H. Lee, H. Chae, S. M. Cho, *Org. Electron.* **2010**, *11*, 427–433.

[47] A. Torres, L. G. C. Rego, *J. Phys. Chem. C* **2014**, *118*, 26947–26954.

[48] Y. Shirota, H. Kageyama, *Chem. Rev.* **2007**, *107*, 953–1010.

[49] T. Braukyla, N. Sakai, M. Daskeviciene, V. Jankauskas, E. Kamarauskas, T. Malinauskas, H. J. Snaith, V. Getautis, *Chem. - An Asian J.* **2016**, *11*, 2049–2056.

[50] I. Neogi, S. Jhulki, A. Ghosh, T. J. Chow, J. N. Moorthy, *ACS Appl. Mater. Interfaces* **2015**, *7*, 3298–3305.

[51] I. Neogi, S. Jhulki, A. Ghosh, T. J. Chow, J. N. Moorthy, *Org. Electron.* **2014**, *15*, 3766–3772.

[52] M. Saliba, T. Matsui, J.-Y. Seo, K. Domanski, J.-P. Correa-Baena, M. K. Nazeeruddin, S. M. Zakeeruddin, W. Tress, A. Abate, A. Hagfeldt, et al., *Energy Environ. Sci.* **2016**,

9, 1989–1997.

[53] Z. Tang, S. Uchida, T. Bessho, T. Kinoshita, H. Wang, F. Awai, R. Jono, M. M. Maitani, J. Nakazaki, T. Kubo, et al., *Nano Energy* **2018**, *45*, 184–192.

[54] C. Wang, C. Zhang, S. Wang, G. Liu, H. Xia, S. Tong, J. He, D. Niu, C. Zhou, K. Ding, et al., *Sol. RRL* **2018**, *2*, 1700209.

[55] M. Deepa, M. Salado, L. Calio, S. Kazim, S. M. Shivaprasad, S. Ahmad, *Phys. Chem. Chem. Phys.* **2017**, *19*, 4069–4077.

[56] K. T. Cho, O. Trukhina, C. Roldán-Carmona, M. Ince, P. Gratia, G. Grancini, P. Gao, T. Marszalek, W. Pisula, P. Y. Reddy, et al., *Adv. Energy Mater.* **2017**, *7*, 1601733.

[57] K. Rakstys, A. Abate, M. I. Dar, P. Gao, V. Jankauskas, G. Jacopin, E. Kamarauskas, S. Kazim, S. Ahmad, M. Grätzel, M. K. Nazeeruddin, *J. Am. Chem. Soc.* **2015**, *137*, 16172.

[58] Y. Shao, Z. Xiao, C. Bi, Y. Yuan, J. Huang, *Nat. Commun.* **2014**, *5*, 5784.

[59] A. K. Jena, M. Ikegami, T. Miyasaka, *ACS Energy Lett.* **2017**, *2*, 1760–1761.

[60] E. Kasparavicius, A. Magomedov, T. Malinauskas, V. Getautis, *Chem. Eur. J.* **2018**, *24*, 9910–9918.

[61] A. Magomedov, E. Kasparavičius, K. Rakstys, S. Paek, N. Gasilova, K. Genevičius, G. Juška, T. Malinauskas, M. K. Nazeeruddin, V. Getautis, *J. Mater. Chem. C* **2018**, *6*, 8874–8878.

[62] A. Abate, T. Leijtens, S. Pathak, J. Teuscher, R. Avolio, M. E. Errico, J. Kirkpatrik, J. M. Ball, P. Docampo, I. McPherson, H. J. Snaith, *Phys. Chem. Chem. Phys.* **2013**, *15*, 2572.

[63] M. Saliba, J. P. Correa-Baena, C. M. Wolff, M. Stolterfoht, N. Phung, S. Albrecht, D. Neher, A. Abate, *Chem. Mater.* **2018**, *30*, 4193.

A hole transporting material termed **V1160**, based on four TPD-type fragments connected by a Tröger's base structural core, was synthesized, characterized, and applied as a HTM in perovskite solar cells. Demonstrating over 18% power conversion efficiency, the fully amorphous nature of **V1160**, suggesting further studies in TPD-based materials are warranted.

Hole transporting materials

T. Braukyla, R. Xia, T. Malinauskas, M. Daskeviciene, A. Magomedov, E. Kamarauskas, V. Jankauskas, Z. Fei, C. Roldán-Carmona, M. Khaja Nazeeruddin*, P. J. Dyson*, V. Getautis*

Application of a Tetra-TPD-type HTM Fused by a Tröger's Base Core in Perovskite Solar Cells.